Commun. Theor. Phys. (Beijing, China) **50** (2008) pp. 111–116

Vol. 50, No. 1, July 15, 2008

Function Projective Synchronization of Discrete-Time Chaotic and Hyperchaotic Systems Using Backstepping Method*

JIN Yi-Liang,[1,3] LI Xin,[2,3] and CHEN Yong[1,3,†]

[1]Nonlinear Science Center and Department of Mathematics, Ningbo University, Ningbo 315211, China

[2]Department of Mathematics, Changshu Institute of Technology, Changshu 215500, China

[3]Key Laboratory of Mathematics Mechanization, the Chinese Academy of Sciences, Beijing 100080, China

(Received October 9, 2007; Revised December 29, 2007)

Abstract *In this paper, a function projective synchronization scheme is developed to investigate the function projective synchronization between the discrete-time driven chaotic system and the discrete-time response chaotic system. With the aid of symbolic-numeric computation, we use the scheme to study the function projective synchronization between 2D Lorenz discrete-time system and Hénon discrete-time system, as well as that between 3D discrete-time hyperchaotic system and Hénon-like map via three scalar controllers, respectively. Moreover numerical simulations are used to verify the effectiveness of the proposed scheme.*

PACS numbers: 05.45.Xt
Key words: discrete-time chaotic system, discrete-time chaotic map, symbolic-numeric computation, function projective synchronization, backstepping design

1 Introduction

Since Lorenz[1] presented the well-known Lorenz chaotic system and Rössler[2] first introduced the Rössler hyperchaotic system, many chaotic systems have been reported in nonlinear field. In particular, since the pioneering works of Fujisaka and Yamada,[3] Pecora and Carroll,[4] Ott, Pyragas,[5] Grebogi and Yorke,[6] chaos (hyperchaos) synchronization has played significant roles because of its potential applications in secure communication. Up to now, many types of chaos synchronization have been presented, such as complete synchronization, partial synchronization, phase synchronization, lag synchronization, anticipated synchronization, generalized slag, anticipated and completed synchronization, antiphase synchronization, etc.[7−13] In particular, amongst all kinds of chaos synchronization, projective synchronization in partial linear systems reported by Mainieri and Rehacek[14] is one of the most noticeable ones that the driven and response vectors evolve in a proportional scale — the vectors become proportional. Some researchers[15−17] extended the projective synchronization to non-partial linear systems, and recently, function projective synchronization (FPS)[18] is proposed in the continuous-time systems, which means the driven and response vectors evolve in a proportional scaling function matrix. Many powerful methods have been reported to investigate some types of chaos (hyperchaotic) synchronization in continuous-time systems. In fact, many mathematical models of neural networks, biological process, physical process and chemical process, etc., were defined using discrete-time dynamical systems.[19−21] Recently, more and more attention was paid to the chaos (hyperchaos) control and synchronization in discrete-time dynamical systems.[22−26]

Recently, in Ref. [27], we presented the definition of function projective synchronization (FPS) in discrete-time dynamical systems, and a systematic and automatic FPS algorithm has been set up to achieve successfully FPS between 2D Lorenz discrete-time system and Fold discrete-time system, as well as between 3D hyperchaotic Rössler discrete-time system and Hénon-like map. Here, the FPS algorithm is developed to make FPS between 2D discrete-time Lorenz system and Hénon system, as well as the 3D discrete-time hyperchaotic system due to Wang[28] and the Hénon-like map. Moreover numerical simulations are used to verify the effectiveness of the proposed scheme.

The rest of this paper is arranged as follows. In Sec. 2, we first introduce FPS in discrete-time systems and investigate FPS in 2D Lorenz discrete-time dynamical system and Hénon system. In Sec. 3, we investigate FPS between the 3D discrete-time hyperchaotic system and the Hénon-like map. Finally, some conclusions and discussions are given in Sec. 4.

2 Function Projective Synchronization of Discrete-Time Chaotic Systems

Firstly we introduce the FPS in discrete-time systems, and then we use Lyapunov stability theory to realize our scheme.

*The project supported by National Natural Science Foundation of China under Grant No. 10735030, Shanghai Leading Academic Discipline Project under Grant No. B412, Natural Science Foundation of Zhejiang Province of China under Grant No. Y604056, the Doctoral Foundation of Ningbo City under Grant No. 2005A61030, the Program for Changjiang Scholars and Innovative Research Team in Universities under Grant No. IRT0734, and K.C. Wong Magna Fund in Ningbo University

†E-mail: chenyong@nbu.edu.cn

Definition For two discrete-time (chaotic or hyperchaotic) dynamical systems,

(i) $x(k+1) = F(x(k))$,

(ii) $y(k+1) = G(y(k)) + u(x(k), y(k))$,

where $(x(k), y(k)) \in R^{m+m}$, $k \in Z/Z^-$, $u(x(k), y(k)) \in R^m$, let

(iii)

$$E(k) = (E_1(k), E_2(k), \ldots, E_m(k)) = (x_1(k) - f_1(x(k))y_1(k), x_2(k) - f_2(x(k))y_2(k), \ldots, x_m(k) - f_m(x(k))y_m(k))$$

be boundary vector functions. If there exist proper controllers

$$u(x(k), y(k)) = (u_1(x(k), y(k)), u_2(x(k), y(k)), \ldots, u_m(x(k), y(k)))^{\mathrm{T}}$$

such that $\lim_{k\to\infty}(E(k)) = 0$, we say that there exists **function projective synchronization (FPS)**.

In the following, using the backstepping method and based on Lyapunov stability theory, FPS of 2D Lorenz discrete-time system and Hénon discrete-time system is realized step by step.

Consider Lorenz discrete-time system

$$x_1(k+1) = (1+\alpha\beta)x_1(k) - \beta x_1(k)x_2(k)\,,\quad x_2(k+1) = (1-\beta)x_2(k) + \beta x_1^2(k)\,, \tag{1}$$

and Hénon system with controllers $u(x, y)$,

$$y_1(k+1) = y_2(k) + 1 - ay_1(k)^2 + u_1(x, y)\,,\quad y_2(k+1) = by_1(k) + u_2(x, y)\,, \tag{2}$$

as the driven system and response system, respectively.

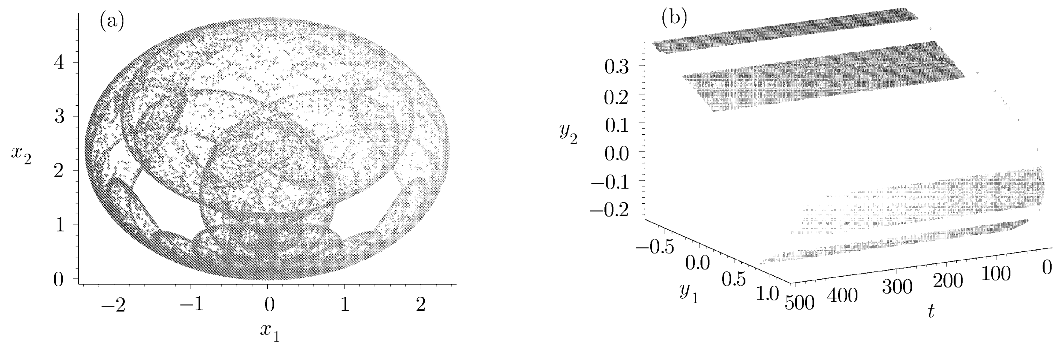

Fig. 1 (a) Lorenz discrete-time attractor; (b) Hénon discrete-time attractor.

Firstly we give the figures (Figs. 1(a) and 1(b)) of the two systems with initial variables $[x_1(0) = 0.1, x_2(0) = 0.2]$ and $[y_1(0) = 0.7, y_2(0) = 0.2]$, respectively. Here $\alpha = 1.25$, $\beta = 0.75$, $a = 1.07$, and $b = 0.3$. In the following, we would like to realize the FPS of Lorenz discrete-time system and Hénon discrete-time system by backstepping design method. We choose

$$(f_1(x), f_2(x)) = \Big(1 + \tanh(x_1(k))^2 + \frac{1}{2}\tanh(x_2(k)), 1 + \tanh(x_2(k))^2\Big)\,,\quad (f_1(x), f_2(x)) = \Big(\frac{1}{2}, \frac{1}{2}\Big)\,,$$

respectively. (i) Let the error states be

$$E_1(k) = x_1(k) - \Big(1 + \tanh(x_1(k))^2 + \frac{1}{2}\tanh(x_2(k))\Big)y_1(k)\,,\quad E_2(k) = x_2(k) - (1 + \tanh(x_2(k))^2)y_2(k)\,.$$

Here we choose $f_1(x) = 1 + \tanh(x_1(k))^2 + (1/2)\tanh(x_2(k))$, $f_2(x) = 1 + \tanh(x_2(k))^2$. Then from Eqs. (1) and (2), we have the discrete-time error dynamical system

$$\begin{aligned} E_1(k+1) &= (1+\alpha\beta)x_1(k) - \beta x_1(k)x_2(k) - \Big(1 + \tanh((1+\alpha\beta)x_1(k) - \beta x_1(k)x_2(k))^2 \\ &\quad + \frac{1}{2}\tanh((1-\beta)x_2(k) + \beta x_1(k)^2)\Big)(y_2(k) + 1 - ay_1(k)^2 + u_1(x, y))\,, \\ E_2(k+1) &= (1-\beta)x_2(k) + \beta x_1(k)^2 - (1 + \tanh((1-\beta)x_2(k) + \beta x_1(k)^2)^2)(by_1(k) + u_2(x, y))\,. \end{aligned} \tag{3}$$

In the following, based on the backstepping design and the improved ideas of Refs. [23] and [26], we give a systematic and constructive algorithm to derive the controllers $u(x, y)$ step by step such that systems (1) and (2) are synchronized together.

Step 1 Let the first partial Lyapunov function be $L_1(k) = |E_1(k)|$ and the second error variable be

$$E_2(k) = E_1(k+1) - c_{11}E_1(k)\,, \tag{4}$$

where $c_{11} \in R$. Then we have the derivative of $L_1(k)$

$$\Delta L_1(k) = |E_1(k+1)| - |E_1(k)| \le (|c_{11}| - 1)|E_1(k)| + |E_2(k)|\,. \tag{5}$$

Step 2 Let

$$E_2(k+1) - c_{21}E_1(k) - c_{22}E_2(k) = 0\,. \tag{6}$$

Then with the aid of symbolic computation, from the above equations (4) and (6) we obtained the controllers,

$$\begin{aligned}u_1(x,y) =\ & (2x_1(k)+2x_1(k)\alpha\beta-2\beta x_1(k)x_2(k)-2+2ay_1(k)^2-2\tanh(x_1(k)+x_1(k)\alpha\beta\\&-\beta x_1(k)x_2(k))^2y_2(k)-2\tanh(x_1(k)+x_1(k)\alpha\beta-\beta x_1(k)x_2(k))^2+2\tanh(x_1(k)\\&+x_1(k)\alpha\beta-\beta x_1(k)x_2(k))^2ay_1(k)^2+\tanh(-x_2(k)+x_2(k)\beta-\beta x_1(k)^2)y_2(k)\\&+\tanh(-x_2(k)+x_2(k)\beta-\beta x_1(k)^2)-\tanh(-x_2(k)+x_2(k)\beta-\beta x_1(k)^2)ay_1(k)^2\\&-2c_{11}x_1(k)+2c_{11}y_1(k)+2c_{11}y_1(k)\tanh(x_1(k))^2+c_{11}y_1(k)\tanh(x_2(k))-2x_2(k)\\&+2y_2(k)\tanh(x_2(k))^2)/(2+2\tanh(x_1(k)+x_1(k)\alpha\beta-\beta x_1(k)x_2(k))^2\\&-\tanh(-x_2(k)+x_2(k)\beta-\beta x_1(k)^2))\,,\\u_2(x,y) =\ & -(1/2)(-2x_2(k)+2x_2(k)\beta-2\beta x_1(k)^2+2by_1(k)+2\tanh(-x_2(k)\\&+x_2(k)\beta-\beta x_1(k)^2)^2by_1(k)+2c_{21}x_1(k)-2c_{21}y_1(k)-2c_{21}y_1(k)\\&\times\tanh(x_1(k))^2-c_{21}y_1(k)\tanh(x_2(k))+2c_{22}x_1(k)-2c_{22}y_1(k)-2c_{22}y_1(k)\\&\times\tanh(x_1(k))^2-c_{22}y_1(k)\tanh(x_2(k)))/(\tanh(-x_2(k)+x_2(k)\beta-\beta x_1(k)^2)^2+1)\,.\end{aligned}\tag{7}$$

Let the second partial Lyapunov function be $L_2(k) = L_1(k)+d_1|E_2(k)|$, where $d_1>1$, then the derivative of $L(k)$ is

$$\begin{aligned}\Delta L(k) &= L_2(k+1)-L_2(k)\\&=\Delta L_1(k)+d_1(|E_2(k+1)|-|E_2(k)|)\\&\le(|c_{11}|-1+d_1|c_{21}|)|E_1(k)|\\&\quad+(1-d_1+d_1|c_{22}|)|E_2(k)|\,.\end{aligned}\tag{8}$$

It follows that the right-hand side of Eq. (8) is negative-definite, if the following conditions hold

$$|c_{11}|+d_1|c_{21}|<1\,,\quad d_1-d_1|c_{22}|>1\,.\tag{9}$$

Obviously, there exist many sets of solutions $[c_{11}, c_{21}, c_{22}]$ that satisfy Eq. (9).

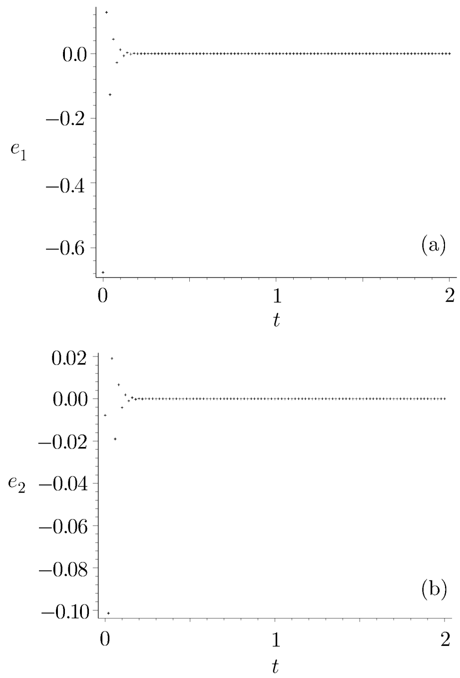

Fig. 2 The orbits of the error states.

In the following we use numerical simulations to verify the effectiveness of the above-mentioned controllers. The parameters are chosen as $d_1 = 2$, $c_{11} = -0.2$, $c_{21} = -0.25$, $c_{22} = 0.4$, and the initial values of systems (1) and (2) with $u = 0$ are taken as those in Fig. 1. The graphs of FPS error states and the globally picture of the driven and response systems are displayed in Figs. 2(a) and 2(b) and Fig. 3.

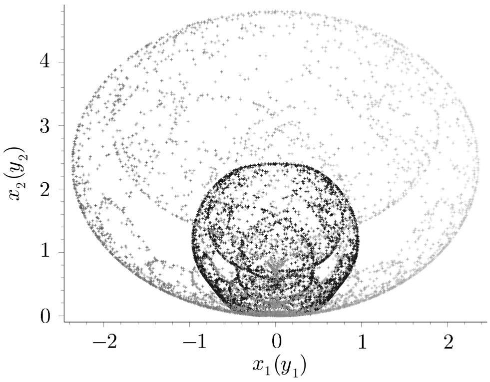

Fig. 3 The two attractors after being synchronized with $(f_1(x), f_2(x)) = (1+\tanh(x_1(k))^2 + (1/2)\tanh(x_2(k)), 1+\tanh(x_2(k))^2)$: the dark one is the response system with the controllers, and the other is the driven system.

3 FPS of 3D Discrete-Time Hyperchaotic System and Hénon-like Map

In this section, we would like to realize the FPS of 3D discrete-time hyperchaotic system due to Wang[28]

$$\begin{aligned}x_1(k+1)&=0.5\delta x_2(k)+(-2.3\delta+1)x_1(k)\,,\\x_2(k+1)&=0.2\delta x_3(k)-1.9\delta x_1(k)+x_2(k)\,,\\x_3(k+1)&=2\delta-0.6\delta x_2(k)x_3(k)+(-1.9\delta+1)x_3(k)\,,\end{aligned}\tag{10}$$

and the 3D Hénon-like discrete-time map

$$\begin{aligned}y_1(k+1)&=1+y_3(k)-\alpha y_2^2(k)+u_1(x,y)\,,\\y_2(k+1)&=1+\beta y_2(k)-\alpha y_1^2(k)+u_2(x,y)\,,\\y_3(k+1)&=\beta y_1(k)+u_3(x,y)\,,\end{aligned}\tag{11}$$

as the driven system and response system, respectively.

Firstly we give the figures (Figs. 4(a) and 4(b)) of the two systems with initial variables $[x_1(0) = 0.05, x_2(0) = 0.03, x_3(0) = 0.02]$ and $[y_1(0) = -0.5, y_2(0) = 0.2, y_3(0) = 0.1]$, respectively. Here $\delta = 1$, and $\alpha = 1.4$, $\beta = 0.2$.

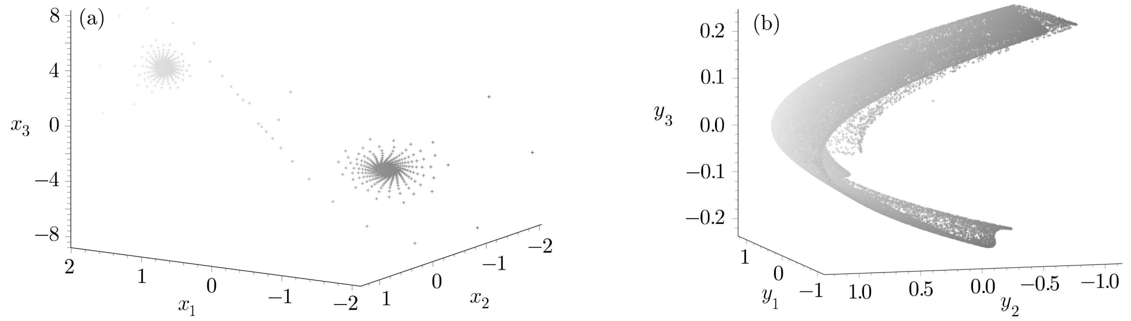

Fig. 4 (a) The attractor of discrete-time hyperchaotic system due to Wang; (b) the attractor of Hénon map.

To realize the synchronization, let the error states be

$$E_1(k) = x_1(k) - \frac{1}{2}(1+\tanh(x_1(k))^2)y_1(k)\,, \quad E_2(k) = x_2(k) - \frac{1}{2}y_2(k)\,, \quad E_3(k) = x_3(k) - \frac{1}{2}y_3(k)\,.$$

Then from Eqs. (10) and (11), we can have the discrete-time error dynamical system,

$$\begin{aligned} E_1(k+1) &= 0.5\delta x_2(k) + (-2.3\delta+1)x_1(k) - 0.5(1+\tanh(0.5\delta x_2(k) \\ &\quad + (-2.3\delta+1)x_1(k))^2)(1+y_3(k) - \alpha y_2(k)^2 + u_1(x,y))\,, \\ E_2(k+1) &= 0.2\delta x_3(k) - 1.9\delta x_1(k) + x_2(k) - 0.5 - 0.5\beta y_2(k) + 0.5\alpha y_1(k)^2 - 0.5u_2(x,y)\,, \\ E_3(k+1) &= 2\delta - 0.6\delta x_2(k)x_3(k) + (-1.9\delta+1)x_3(k) - 0.5\beta y_1(k) - 0.5u_3(x,y)\,. \end{aligned} \tag{12}$$

Based on the backstepping design method and Lyapunov stability theory, we can get the controllers step by step like the situation in Sec. 3. Here we omit the concrete process. Finally, with the aid of symbolic computation, from

$$\begin{aligned} &E_1(k) = x_1(k) - \frac{1}{2}(1+\tanh(x_1(k))^2)y_1(k)\,, \quad E_2(k) = E_1(k) - c_{11}E_1(k)\,, \\ &E_3(k) = E_2(k+1) - c_{21}E_1(k) - c_{22}E_2(k)\,, \quad E_3(k+1) - c_{31}E_1(k) - c_{32}E_2(k) - c_{33}E_3(k) = 0\,, \end{aligned} \tag{13}$$

we can get the controllers $u_1(x,y)$, $u_2(x,y)$, and $u_3(x,y)$:

$$\begin{aligned} u_1(x,y) &= 0.2(5\delta x_2(k) - 23\delta x_1(k) + 10x_1(k) - 5 - 5y_3(k) + 5\alpha y_2(k)^2 - 5\tanh(-0.5\delta x_2(k) \\ &\quad + 2.3\delta x_1(k) - x_1(k))^2 - 5\tanh(-0.5\delta x_2(k) + 2.3\delta x_1(k) - x_1(k))^2 y_3(k) \\ &\quad + 5\tanh(-0.5\delta x_2(k) + 2.3\delta x_1(k) - x_1(k))^2\alpha y_2(k)^2 - 10c_{11}x_1(k) + 5c_{11}y_1(k) \\ &\quad + 5c_{11}y_1(k)\tanh(x_1(k))^2 - 10x_2(k) + 5y_2(k))/(\tanh(-0.5\delta x_2(k) + 2.3\delta x_1(k) - x_1(k))^2 + 1)\,, \\ u_2(x,y) &= 0.4\delta x_3(k) - 3.8\delta x_1(k) + 2x_2(k) - 1 - \beta y_2(k) + \alpha y_1(k)^2 - 2c_{21}x_1(k) + c_{21}y_1(k) \\ &\quad + c_{21}y_1(k)\tanh(x_1(k))^2 - 2c_{22}x_2(k) + c_{22}y_2(k) - 2x_3(k) + y_3(k)\,, \\ u_3(x,y) &= 4\delta - 1.2\delta x_2(k)x_3(k) - 3.8\delta x_3(k) + 2x_3(k) - \beta y_1(k) - 2c_{31}x_1(k) + c_{31}y_1(k) \\ &\quad + c_{31}y_1(k)\tanh(x_1(k))^2 - 2c_{32}x_2(k) + c_{32}y_2(k) - 2c_{33}x_3(k) + c_{33}y_3(k)\,. \end{aligned} \tag{14}$$

Let the Lyapunov function be $L(k) = |E_1(k)| + d_1|E_2(k)| + d_2|E_3(k)|$, $d_2 > d_1 > 1$. Then from Eqs. (13), we obtain the derivative of the Lyapunov function $L(k)$

$$\begin{aligned} \Delta L(k) = L(k+1) - L(k) &\le (d_2|c_{31}| + d_1|c_{21}| + |c_1 1| - 1)|E_1(k)| + (d_2|c_{32}| + d_1(|c_{22}| - 1) + 1)|E_2(k)| \\ &\quad + (d_2|c_{33}| + d_1 - d_2)|E_3(k)|\,. \end{aligned} \tag{15}$$

If we set these constants c_{11}, c_{21}, c_{22}, c_{31}, c_{32}, c_{33} to satisfy

$$d_1|c_{21}| + d_2|c_{31}| + |c_{11}| < 1\,, \quad d_1|c_{22}| + d_2|c_{32}| < d_1 - 1\,, \quad |c_{33}| < \frac{d_2 - d_1}{d_2}\,, \tag{16}$$

then $\Delta L(k)$ is negative-definite, which denotes that the resulting close-loop discrete-time system

$$\begin{pmatrix} E_1(k+1) \\ E_2(k+1) \\ E_3(k+1) \end{pmatrix} = \begin{pmatrix} c_{11} & 1 & 0 \\ c_{21} & c_{22} & 1 \\ c_{31} & c_{32} & c_{33} \end{pmatrix} \begin{pmatrix} E_1(k) \\ E_2(k) \\ E_3(k) \end{pmatrix} \tag{17}$$

is globally asymptotically stable and $\lim_{k\to+\infty} E_i(k) = 0$, that is to say, hyperchaotic 3D discrete-time hyperchaotic system due to Wang[28] (10) and the Hénon-like map (11) are function projective synchronized.

In the following we use numerical simulations to verify the effectiveness of the obtained controllers $u(x,y)$. Here we take $c_{11} = 0.3$, $c_{21} = 0.02$, $c_{22} = 0.4$, $c_{31} = 0.05$, $c_{32} = 0.1$, $c_{33} = -0.2$, $d_1 = 4$, $d_2 = 6$, and the initial values

$[x_1(0) = 0.05, x_2(0) = 0.03, x_3(0) = 0.02]$ and $[y_1(0) = -0.5, y_2(0) = 0.2, y_3(0) = 0.1]$, respectively. The graphs of the error states are shown in Figs. 5(a) $\sim$ 5(c), and the attractors of the two systems with controllers are displayed in Fig. 6.

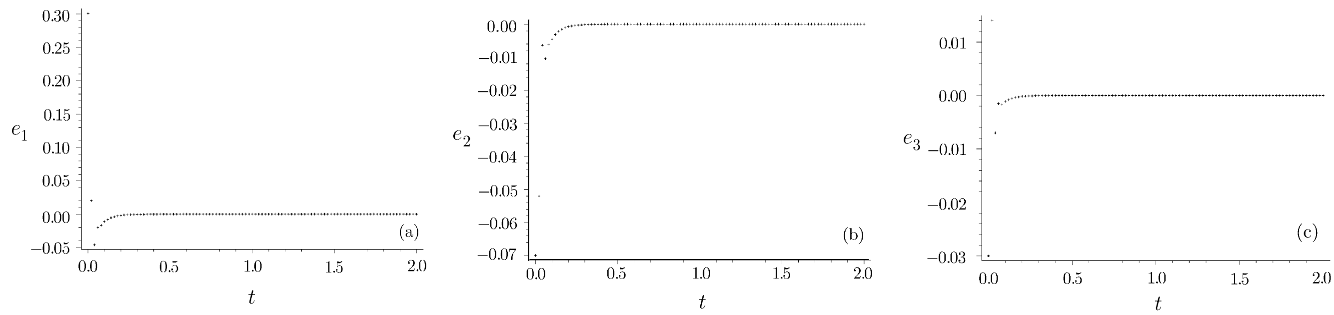

Fig. 5 The orbits of the error states.

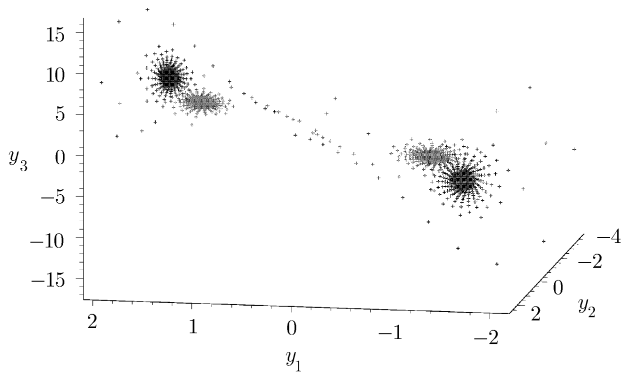

Fig. 6 The two attractors after being synchronized with $(f_1(x), f_2(x), f_3(x)) = (\frac{1}{2}(1 + \tanh(x_1(k))^2), \frac{1}{2}, \frac{1}{2})$: the dark one is the response system with the controllers, and the other is the driven system.

4 Summary and Conclusion

In summary, based on backstepping method and Lyapunov stability theory, a systematic and automatic scheme is developed to investigate FPS between the discrete-time driven systems and response systems: between the 2D discrete-time Lorenz system and Hénon system, as well as the 3D discrete-time hyperchaotic system and the Hénon-like map. Numerical simulations show the effectiveness of the proposed scheme. Some interesting figures are drown to show the FPS between different discrete-time systems. In addition, the scheme can also be applied to investigate the tracking problem in the discrete-time systems and to generate automatically the scalar controller in computer with the aid of symbolic-numeric computation.

References

[1] E.N. Lorenz, J. Atmos. Sci. **20** (1963) 130.

[2] O.E. Rössler, Phys. Lett. A **71** (1979) 397.

[3] H. Fujisaka and T. Yamada, Prog. Theor. Phys. **69** (1983) 32.

[4] L.M. Pecora and T.L. Caroll, Phys. Rev. Lett. **64** (1990) 821; T.L. Caroll and L.M. Pecora, IEEE Trans. Circuits Syst., I: Fundam. Theory Appl. **38** (1991) 453.

[5] K. Pyragas, Phys. Lett. A **170** (1992) 421; K. Pyragas, Phys. Lett. A **181** (1993) 203.

[6] E. Ott, C. Grebogi, and J.A. Yorke, Phys. Rev. Lett. **64** (1990) 1196.

[7] S. Boccaletti, J. Kurth, G. Osipov, D.L. Valladares, and C.S. Zhou, Phys. Rep. **366** (2002) 1.

[8] L. Kocarev and U. Parlitz, Phys. Rev. Lett. **76** (1996) 1816.

[9] R. Brown and L. Kocarev, Chaos **10** (2000) 344.

[10] S. Boccaletti, L.M. Pecora, and A. Pelaez, Phys. Rev. E **63** (2001) 066219.

[11] T. Kapitaniak, Phys. Rev. E **50** (1994) 1642; T. Kapitaniak, L.O. Chua, and G.Q. Zhong, Int. J. Bifur. Chaos **6** (1996) 211.

[12] G. Chen and X. Dong, *From Chaos to Order*, World Scientific, Singapore (1998).

[13] Z.Y. Yan, Chaos **15** (2005) 023902; Z.Y. Yan, Chaos, Solitons and Fractals **26** (2005) 406.

[14] R. Mainieri and J. Rehacek, Phys. Rev. Lett. **82** (1999) 3042.

[15] J. Yan and C. Li, Chaos, Solitons and Fractals **26** (2005) 1119.

[16] G. Wen and D. Xu, Chaos, Solitons and Fractals **26** (2005) 71.

[17] G.H. Li, Chaos, Solitons and Fractals **32** (2007) 1454.

[18] Y. Chen and X. Li, Z. Naturforsch. **62a** (2007) 176.

[19] T. Yamakawa, *et al.*, *Proc. of the 2nd International Conference on Fuzzy Logic and Neural Networks*, (1992) pp. 563.

[20] M. Henon, Commun. Math. Phys. **50** (1976) 69; K. Stefanski, Chaos, Solitons and Fractals **9** (1998) 93; G. Baier and M. Klain, Phys. Lett. A **151** (1990) 281; N.F. Rulkov, Phys. Rev. Lett. **86** (2001) 183.

[21] M. Itoh, T. Yang, and L.O. Chua, Int. J. Bifurcation Chaos Appl. Sci. Eng. **11** (2001) 551; K. Konishi and H. Kokame, Phys. Lett. A **248** (1998) 359; M. Itoh and L.O. Chua, Int. J. Bifurcation Chaos Appl. Sci. Eng. **13** (2003) 1055; J. Douglass, L. Wilkens, E. Pantazelou, and F. Moss, Nature (London) **365** (1993) 337.

[22] G.M. Zaslavsky, M. Edelman, and B.A. Niyazov, Chaos **7** (1997) 159; A. Becker and P. Eckelt, Chaos **3** (1993) 487; M. Itoh, *et al.*, IEICE Trans. Fundamentals E **77** (1994) 2092.

[23] Z.Y. Yan, Chaos **16** (2006) 013119; Z.Y. Yan, Phys. Lett. A **342** (2005) 309.

[24] I. Kanellakopoulos, P.V. Kokotovic, and A.S. Morse, IEEE Trans. Autom. Control **36** (1991) 1241.

[25] M. Krstic, *et al.*, *Nonlinear Adaptive Control Design*, Wiley, New York (1995).

[26] C. Wang and S.S. Ge, Chaos, Solitons and Fractals **12** (2001) 1199.

[27] Q. Wang and Y. Chen, Appl. Math. Comp. **181** (2006) 48.

[28] X.Y. Wang, *Chaos in Complex Nonlinear Systems*, Electronics Industry Press, Beijing (2003).